

**Original Article**

# **ADVANCING MOTOR EFFICIENCY: ENHANCING INDUCTION MOTOR FUNCTIONALITY WITH CIRCULAR FLUX TRAJECTORIES IN DIRECT TORQUE CONTROL**

*Emily Carter*

Department of Electrical Engineering,  
University of Michigan, USA

**Abstract:** Induction machines have long held a pivotal role as robust and reliable workhorses within the industrial landscape, making them the prime choice for motor-driven applications. The prevalence of induction motor control drives in global markets underscores their dominance. This paper delves into the intricacies of controlling induction motor drives powered by voltage source inverters instead of the traditional three-phase main source. This approach offers enhanced control over both electromagnetic torque and stator flux linkage directly and seamlessly. The voltage source inverter facilitates the generation of precisely controlled PWM signals with amplitude governed by the DC link, which are then utilized to synthesize phase voltages. The focal point of this study is the analysis of the mathematical model of AC motors in the stator coordinate system. This framework serves as the basis for exerting control over the motor's flux linkage and torque. By adopting this methodology, the necessity for convoluted transformations and intricate calculations, such as vector rotation transformations, is obviated. Consequently, signal processing is simplified, and the control signals employed enable the observer to discern the physical processes of the AC motor with directness and clarity.

**Keywords:** Induction motor, voltage source inverter, stator flux linkage, electromagnetic torque, space vector.

## **INTRODUCTION**

Induction machines are simple, rugged and are considered to be a workhorse of the industry. Due to this induction motor control drive dominate the world market. Control of induction motor drive supplied by voltage source inverter instead of three phase source comes from main. This mechanism helps us to control both electromagnetic torque and stator flux-linkage easily and directly. The inverter gives us easily controlled generated PWM signals and the amplitude is controlled by DC link. From this, we construct phase voltages. In this paper Analyze the mathematical model of the AC motor directly in the stator coordinate system. Based on this, control the motor's flux linkage and torque. It eliminates complicated transformations and calculations such as vector rotation transformations. Therefore, the signal processing required by it is particularly simple and the control signals used to make it possible for the observer to make a direct and explicit determination of the physical process of the AC motor. The stator flux linkage is used for the magnetic field orientation. As long as the stator resistance is known,

## Original Article

it can be observed. This greatly reduces the control performance in vector control technology and is susceptible to parameter changes. The concept of space vector was used to analyze the mathematical model of the three-phase AC motor and control its physical quantity, making the problem particularly simple and clear. At present, DTC is divided into two different schemes in terms of magnetic flux trajectory: the hexagonal scheme and a circular scheme. Because the induction motor is powered by a three-phase symmetrical sine wave, the air gap magnetic potential of the motor is circular. At this time, the motor loss, torque ripple, and noise are the minima. Therefore, in the medium and low power applications, we are tending to use the circular flux trajectory scheme; The hexagonal scheme is only considered in some high-power areas (switching frequency and switching losses have large limits) not discuss in this paper [1].

### Objective of the Paper

The main objective is to improve the dynamic performance of Induction Motor Drive by implementing a Space Vector Modulation (SVPWM) based VSI fed induction motor drive using MATLAB Simulink.

The overall objectives are:

- To develop the equivalent d-q model of Induction motor in the stationary reference frame for its control analysis and its closed loop operation.
- To design DTC drives with developed induction motor model in the MATLAB/Simulink.
- To Develop and Use the anti-windup PI speed(sensorless) controller program for the purpose of our system to be a closed loop system.
- To develop the estimated speed of an induction motor from the estimated stator variables of an induction motor.

### DTC Drive MATLAB Simulation and Modeling Results and Discussion MATLAB

Simulation analysis of three phase squirrel cage induction motor based on direct torque control drive scheme is simulated using MATLAB 2016a platform. The Simulink modeling contains modeled three-phase induction motor in a stationary reference frame, rotor speed estimator, stator flux linkage estimation block, stator flux controller, stator flux linkage position identifier block, estimated torque block, torque controller, optimal switching table block and voltage source inverter. Various parameters are plotted within a given time interval in seconds. The following are the parameters of three-Phase induction motor used during the simulation.

Table 1: System specification of squirrel cage induction motor

Parameters	Values
Rated power (P)	370watt
Stator resistance ( $R_s$ )	11.05ohm
Rotor resistance ( $R_r$ )	6.11ohm
Stator linkage inductance ( $L_s$ )	0.316423H
Rotor linkage inductance ( $L_r$ )	0.316423H
Mutual inductance ( $L_m$ )	0.293939H

## Original Article

Moment of inertia (J)	0.009kg.m <sup>2</sup>
Number of poles (p)	4
Stator rated current (i <sub>s</sub> )	1.1Amp
Rated frequency (f)	50Hz
Rated electrical(mechanical) rotor speed	2640(1320) rpm
Rated stator phase rms voltage	220volt

Table 2: Base values of IPM voltage source inverter and induction motor

Base parameters	Values
Base phase voltage	220V
Base phase current	10A
Base flux	2.93939 volt-sec/rad
Base frequency	50Hz
Base torque	22.604485 N.M
Switching frequency of IPM	10kHz
Base Dc Bus Voltage	300volt

**Induction Motor Modeling for Simulation Analysis**

Induction machine has nonlinear characteristics by nature. From previous experience induction motor has complicated formulae to drive the expression of voltage, current, flux-linkage, and instantaneous electromagnetic torque and other expressions. However, by using fundamental physical laws and space vector theory we can easily to show that our expression is simplified and it is easy to in terms of controlling, understanding, designing, programming, and analysis. Due to this, the space phasor of various quantity will be discussed and with the help of this space phasor model of induction machine it gives detail explanation of fundamental principles involved in direct torque control machines [1].

Induction motor dynamic model and equation varies with the types of the reference frame we used. Stationary reference frame is the most suitable for our analysis; depend on this three-phase induction motor equivalent circuit in stationary reference frame [2] we got the following stationary reference frame dynamic modeling of the three-phase induction machine.

# Original Article

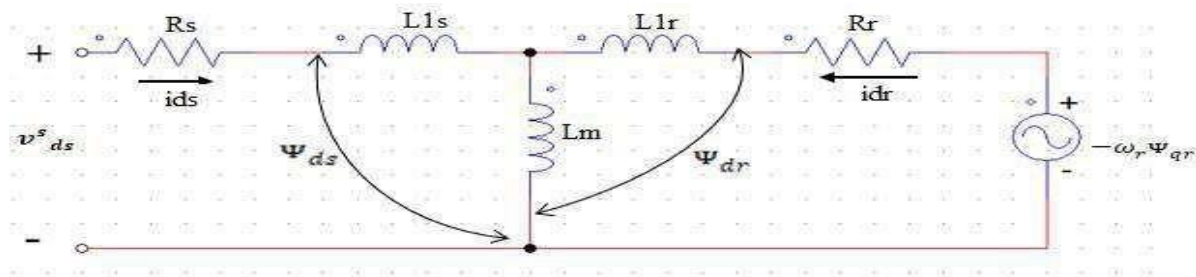


Figure 1: Equivalent circuit in direct axes referred to the stationary reference frame

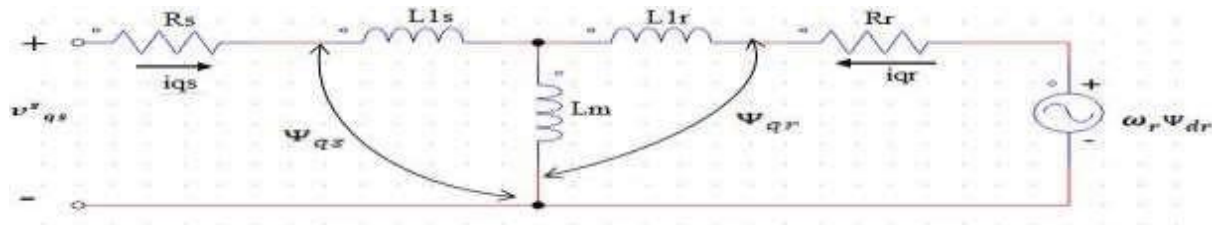


Figure 2: Equivalent circuit in quadrature axes referred to the stationary reference frame

$$v_{ds} = R_s i_{ds} + \frac{d\psi_{ds}}{dt} - \omega_r \psi_{qr} \quad (1)$$

We have also another expression for the above stator voltage equation (1) by substituting the stator flux linkage based on current model equations (2 and 3) [2].

$$\psi_{ds} = L_{ls} i_{ds} + L_m i_{dr} \quad (2)$$

$$\psi_{qs} = L_{ls} i_{qs} + L_m i_{qr} \quad (3)$$

discrete operator,  $T_s$  is the sampling time. By referring equation (1), we can get the following equation forms,

$$\psi_{ds}(t) = \int [v_{ds}(t) - R_s i_{ds}(t)] dt \quad (9)$$

$$\psi_{qs}(t) = \int [v_{qs}(t) - R_s i_{qs}(t)] dt \quad (10)$$

Based on equation above equation (9) and (10), for both equations replace the integral term (1) by  $\frac{T_s}{s}$ . We have the following discrete representation forms of stator flux,

$$\psi_{qs} = T_s (v_{qs} - R_s i_{qs}) \quad (11)$$

$$\psi_{ds} = T_s (v_{ds} - R_s i_{ds})$$

Where  $\psi_{TT-1}$  is the previous value of the stator flux in the q axis, and  $\psi_{TT-1}$  the previous value of the stator flux in d axis. We use a lowpass filter with cutoff frequency  $\frac{1}{3T_s}$  after sampling

# Original Article

stator flux  $\psi_{st}$

$dt$

$T_r$  rotor shaft electrical speed in rad per second.  $T$  is the mechanical rotor speed in rad per second. substituting equation (2 and 3) into the estimated torque equation 12.

Finally, we have the electrical speed equation as and assume load torque is zero:

$$\frac{d\omega_r}{dt} = \frac{1}{J} \left[ \frac{2}{3} \frac{P}{2} \left( \frac{P}{2} \right) \right] \psi_m \quad (8)$$

$\psi$

The above five differential equation (4,5,6,8) is used for the induction machine Simulink model to see the direct torque control drive performance

## Modified Stator Flux Estimator

When we working on digital simulation and implementation, we must change equations from continues to discrete. In a continuous form of an equation, we know Laplace (s) term for derivative, and  $\frac{1}{s}$  for the integral term. In a digital implementation, we also define the

$T$

following based on the types of approximation we used, i.e. backward approximation. Replace  $\frac{1}{s}$  term (the integral term) by  $\frac{1}{s} \approx \frac{T}{1 - e^{-sT}}$  where s is continuous Laplace term and Z is

$$\frac{1}{s} \approx \frac{T}{1 - e^{-sT}}$$

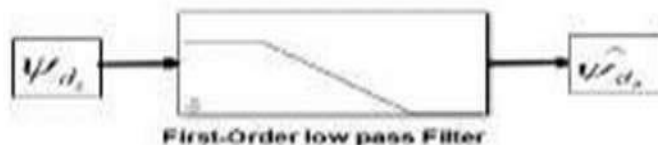


Figure 3: Low pass filter

The transfer function of the lowpass filter is  $\frac{1}{1 + sT}$ ,  $T$  is the suitable time constant, to

$T$

obtain the stator flux at low frequency. the backward approximation can relate the  $T$  and  $\psi$ .  $T = \psi$ , and for q axis flux  $T = \psi$ .

$$\frac{T}{T} = \frac{1 + T}{1 + T} \quad T = \frac{1 + T}{1 + T}$$

## Original Article

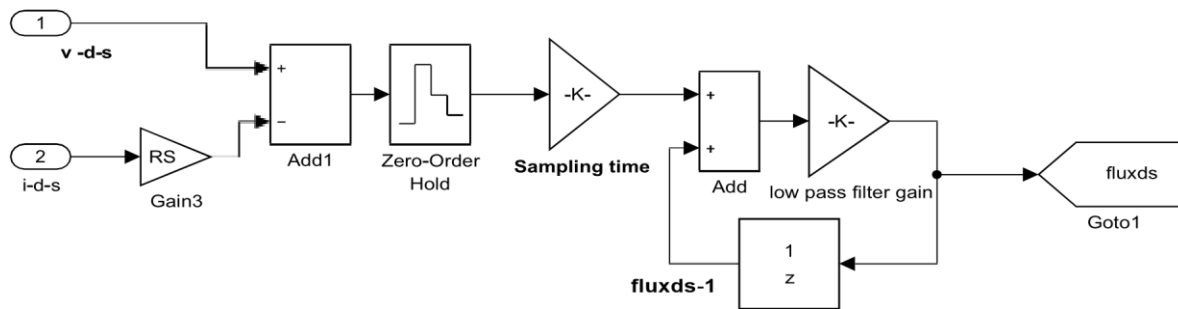


Figure 4: Digital Simulink block diagram for stator d axis flux in a stationary frame

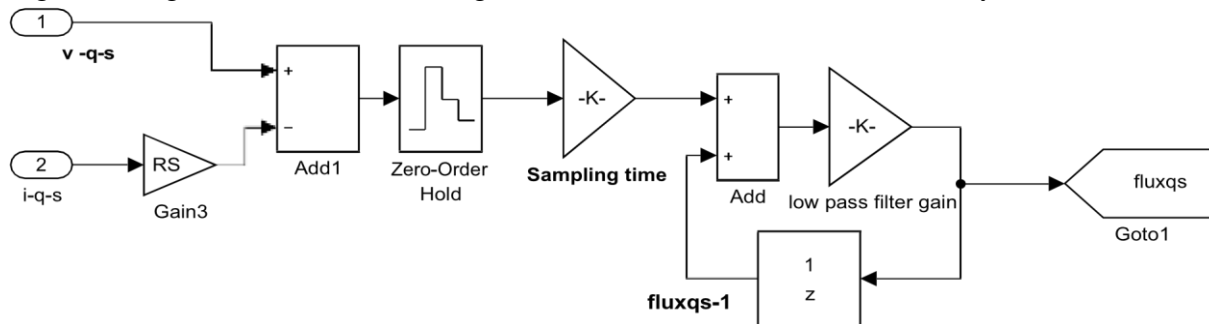


Figure 5: Digital Simulink block diagram for stator q axis flux in the stationary frame

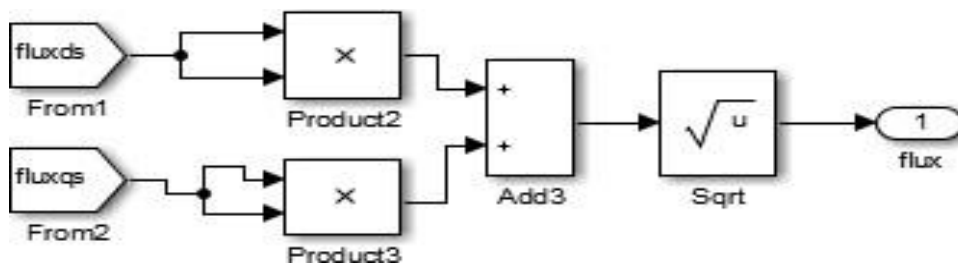


Figure 6: Resultant Stator flux calculation Simulink block

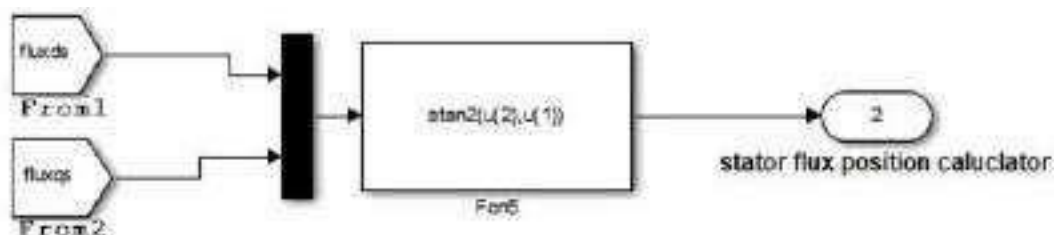


Figure 7: Flux position Simulink block

## Original Article

### Estimating Electromagnetic Torque from Modified Stator Flux

Torque is estimated based on the measured and sensed parameters. Equation (12) is depend on directly from the sensed stator stationary currents and estimated stator stationary flux linkages parameters. So, it reduces the Burdon of the processor during simulation as well as hardware implementation.

$$T_e = \frac{3}{2} p \frac{\lambda_{ds}^* q_s}{\lambda_{qs}^*} i_{qs} \quad (12)$$

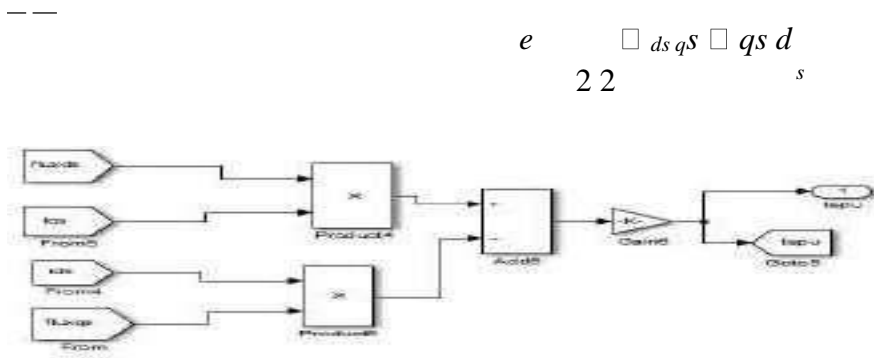


Figure 8: Torque estimator Simulink block

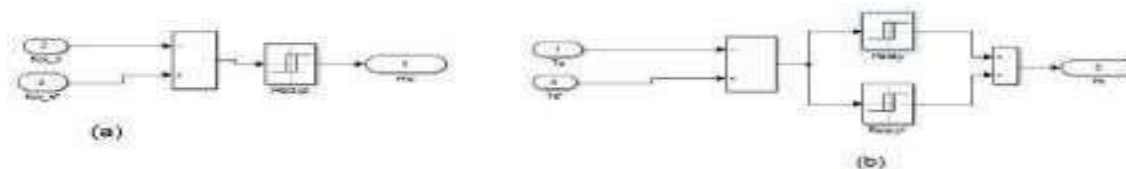


Figure 9: Hysteresis block a) Flux hysteresis controller b) Torque hysteresis controller

### Modified Rotor Speed Estimation Techniques

Rotor Speed sensing technique is using its own estimated and measured electrical output parameters like voltage, current, stator flux linkage, rotor flux linkage, and developed torque. Speed estimation of an induction machine is more complex than other synchronous due to the slip speed. So, for asynchronous machines, we have many tricks for rotor speed estimation. various techniques are described which can be used in high-performance drives for the estimation of the synchronous speed, slip speed, rotor speed, rotor angle, and various machine flux linkages [3]. Thus, in this paper Openloop estimators using monitored stator voltages, currents, and flux linkages is used for the speed estimation;

The main advantages of sensorless-controlled drives are the reduced hardware complexity, the lower cost, the reduced size of the drive machine, the elimination of the sensor cables, the better noise immunity, the increased reliability, and the lower maintenance requirements and lower robustness [4]. Our analysis is in the stationary reference frame fixed to the stator; the differentiation of stator flux angle gives the synchronous speed.

$$\omega_{syn} = \frac{d}{dt} \angle \lambda_s(t) \quad (13)$$

# Original Article

When we differentiate the above equation using the property of inverse tangent function differentiation.

$$\frac{d}{dt} \left[ \frac{\int \omega_{syn} dt}{\int \omega_{syn} dt} \right] = \frac{d}{dt} \left[ \frac{\int \omega_{syn} dt}{\int \omega_{syn} dt} \right] \quad (14)$$

□□

syn 2 s

Equation (14) is not giving us the exact estimated rather it gives disturbed higher frequency noise signal due to modeling error [1]. During digital simulation (implementation), this can be removed by first order low pass filter.

In this paper, we used a low pass filter with cutoff frequency  $\frac{5}{sec} TTT$ .



Figure 10: Low pass filter for synchronous speed estimation

1

$$T_{TTT} = T_{TTT} \frac{1}{1 + TTT} \quad (15)$$

$$\frac{d}{dt} \left[ \frac{\int \omega_{syn} dt}{\int \omega_{syn} dt} \right] = \frac{d}{dt} \left[ \frac{\int \omega_{syn} dt}{\int \omega_{syn} dt} \right] \quad (16)$$

Using backward approximation techniques, equation 16 can be written as by replacing  $\frac{1}{T} = \frac{TTT}{T-1}$ .

$$\frac{d}{dt} \left[ \frac{\int \omega_{syn} dt}{\int \omega_{syn} dt} \right] = \frac{d}{dt} \left[ \frac{\int \omega_{syn} dt}{\int \omega_{syn} dt} \right] \quad (17)$$

The main challenging task during asynchronous machine speed estimation is to obtain slip speed estimation. We have from many tricks of slip speed estimation [1].

2Rr Testimated

$$\frac{d}{dt} \left[ \frac{\int \omega_{syn} dt}{\int \omega_{syn} dt} \right] = \frac{d}{dt} \left[ \frac{\int \omega_{syn} dt}{\int \omega_{syn} dt} \right] \quad (18)$$

Equation (18) slip estimation techniques have simple mathematical analysis and can be easy interims of simulation time and coding from other estimation methods, but it needs resultant rotor flux linkage. So, this rotor flux linkage can be obtained from stator currents and modified estimated stator flux linkage. Also, the main thing we are going to do in this slip estimation techniques, the synchronous speed estimation method also changed from the equation (14). The slip speed is depending on rotor flux linkage speed [1]. Then the rotor speed is estimated as follows. □□



## Original Article

□  $r$  □  $\square_{syn}$  □  $\square_{slip}$ 

(19)

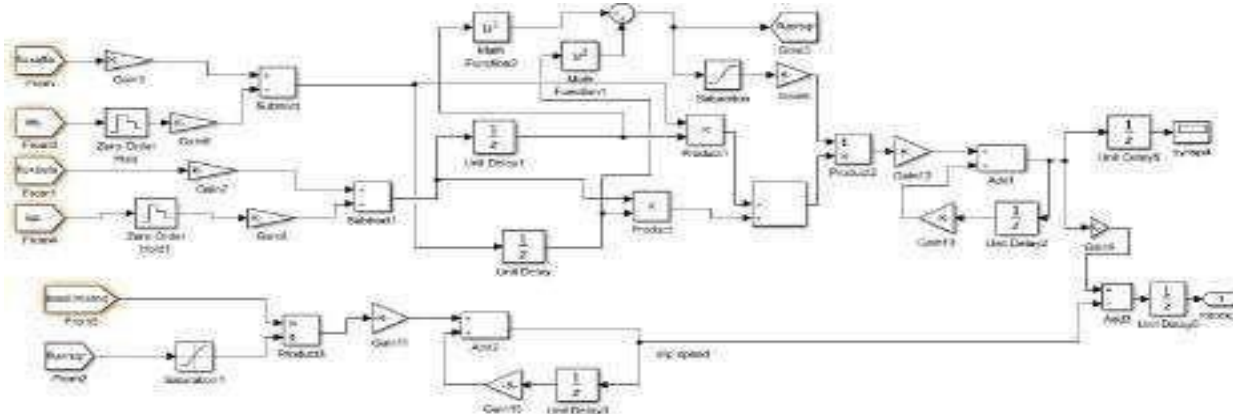


Figure 11: Digital rotor speed estimation using Simulink

**MATLAB Simulation Results**

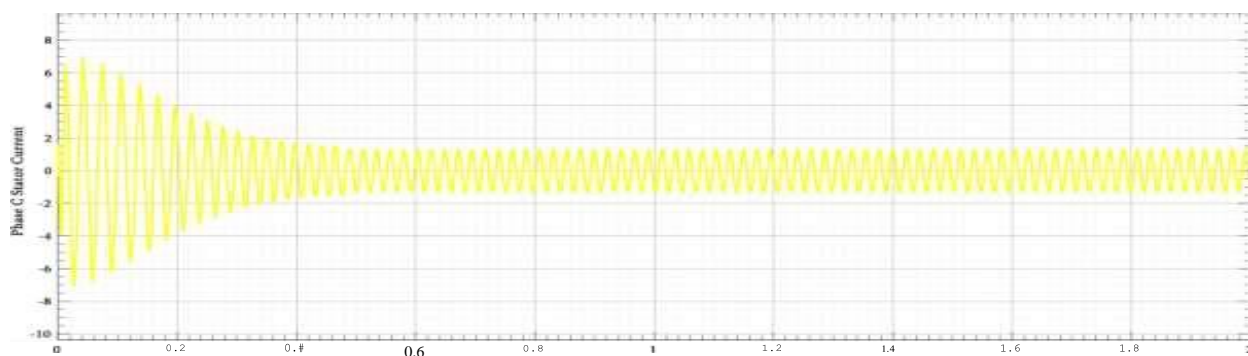
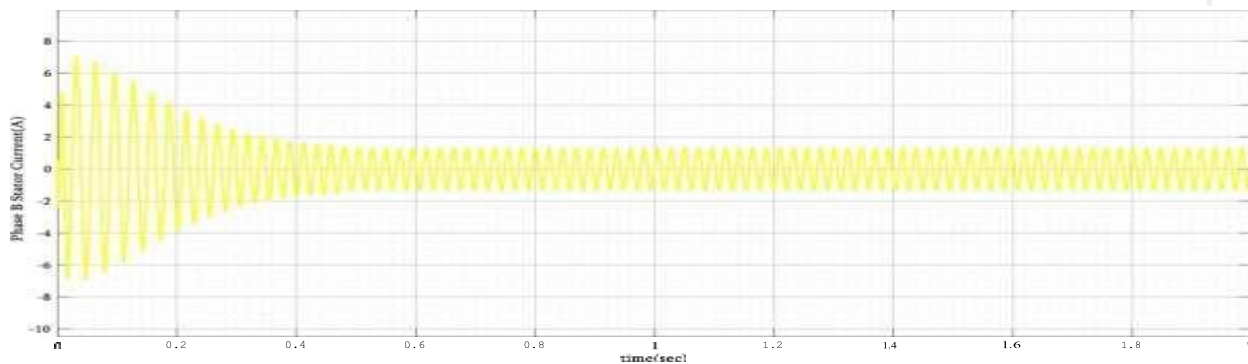
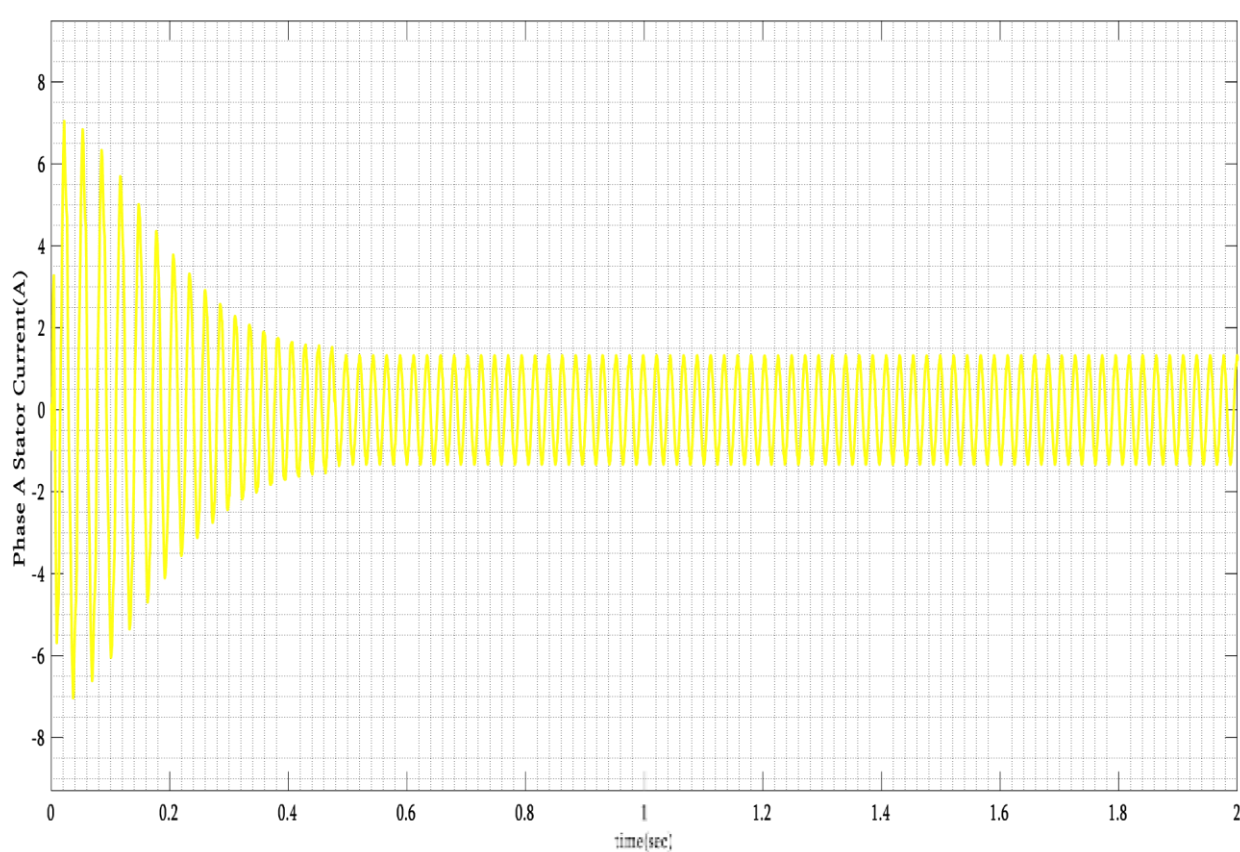
The simulation results are based on Overall MATLAB simulation system presented on figure 12.

The details of each block are presented. The Simulink block generally has the direct torque control IM drive with a closed-loop speed control system using estimated speed as feedback comparing with the reference speed using a PI as a speed controller. The MATLAB plots without load are shown below. The reference values for the different parameter are shown in below table 3.

Table 3. set point values of difference parameter used in simulink

Reference parameter	Values
Stator flux	0.4volt-sec/rad
Rotor Electrical Speed reference	276 rad/sec
KP	50
KI	0.03
VDC (dc bus voltage)	200V

Original Article



## Original Article

Figure 12: Stator three-phase currents MATLAB Simulink results

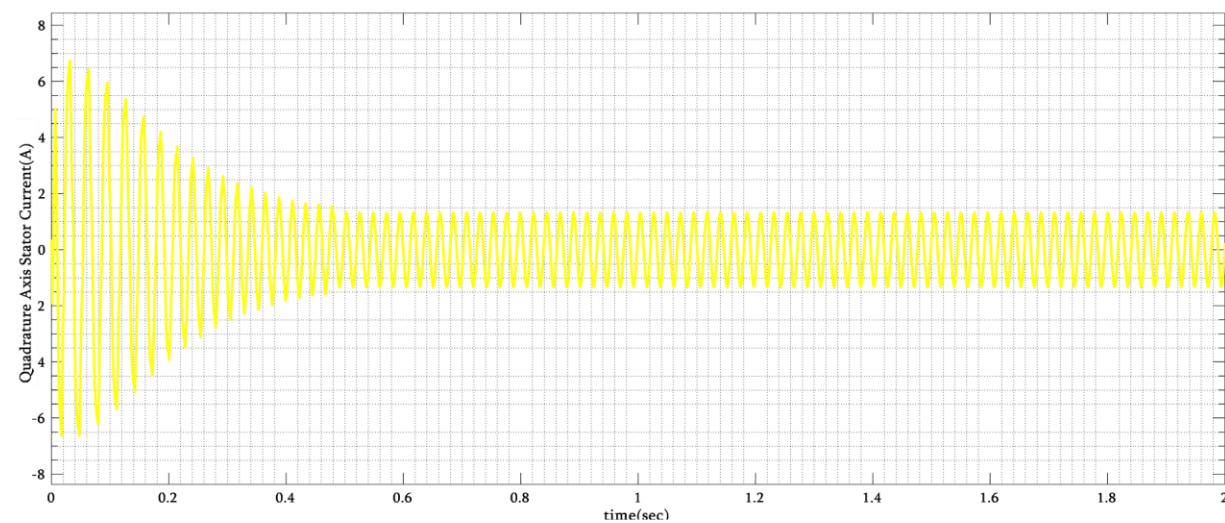
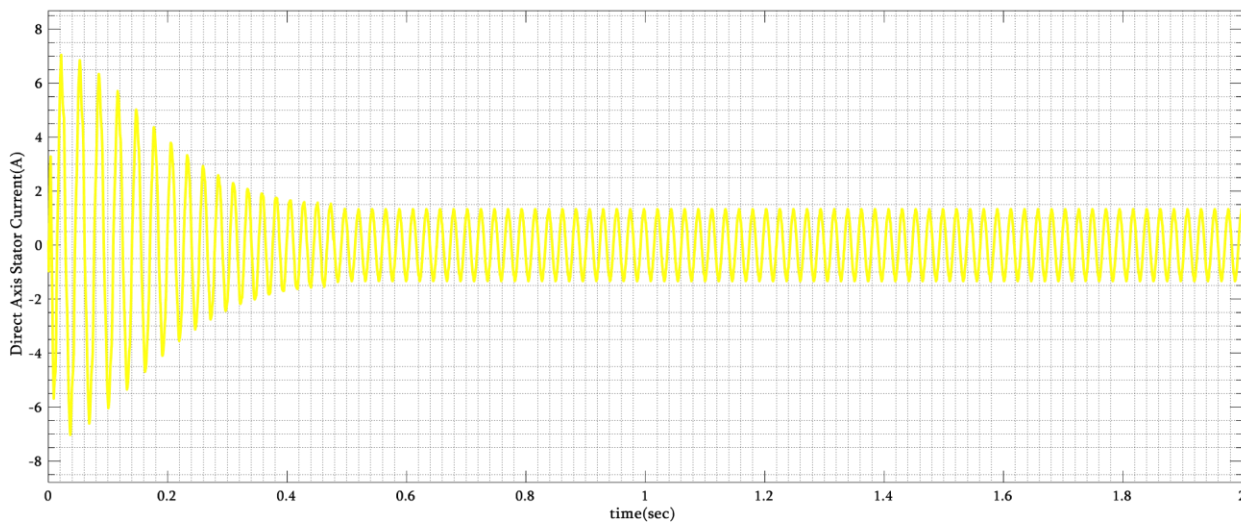


Figure 13: Stationary direct and quadrature axis current

The above plot figure 12 shows that initially the stator phase current has larger value which comes from speed PI controller gains but after some time when it reaches at steady it gets smaller values which almost gives the rating current of the motor. Also, we observe that the three-phase stator winding current has approximately sinusoidal waveforms with constant frequency. We have also the direct and quadrature axis currents as shown in figure 13; the direct axis current almost the same as the stator phase A current and from the figure 13 the angle between the direct and quadrature stator current has  $90^\circ$  phase shifts as expected. We observe this phase shift also in direct and quadrature axis stator flux below in figure 14.

## Original Article

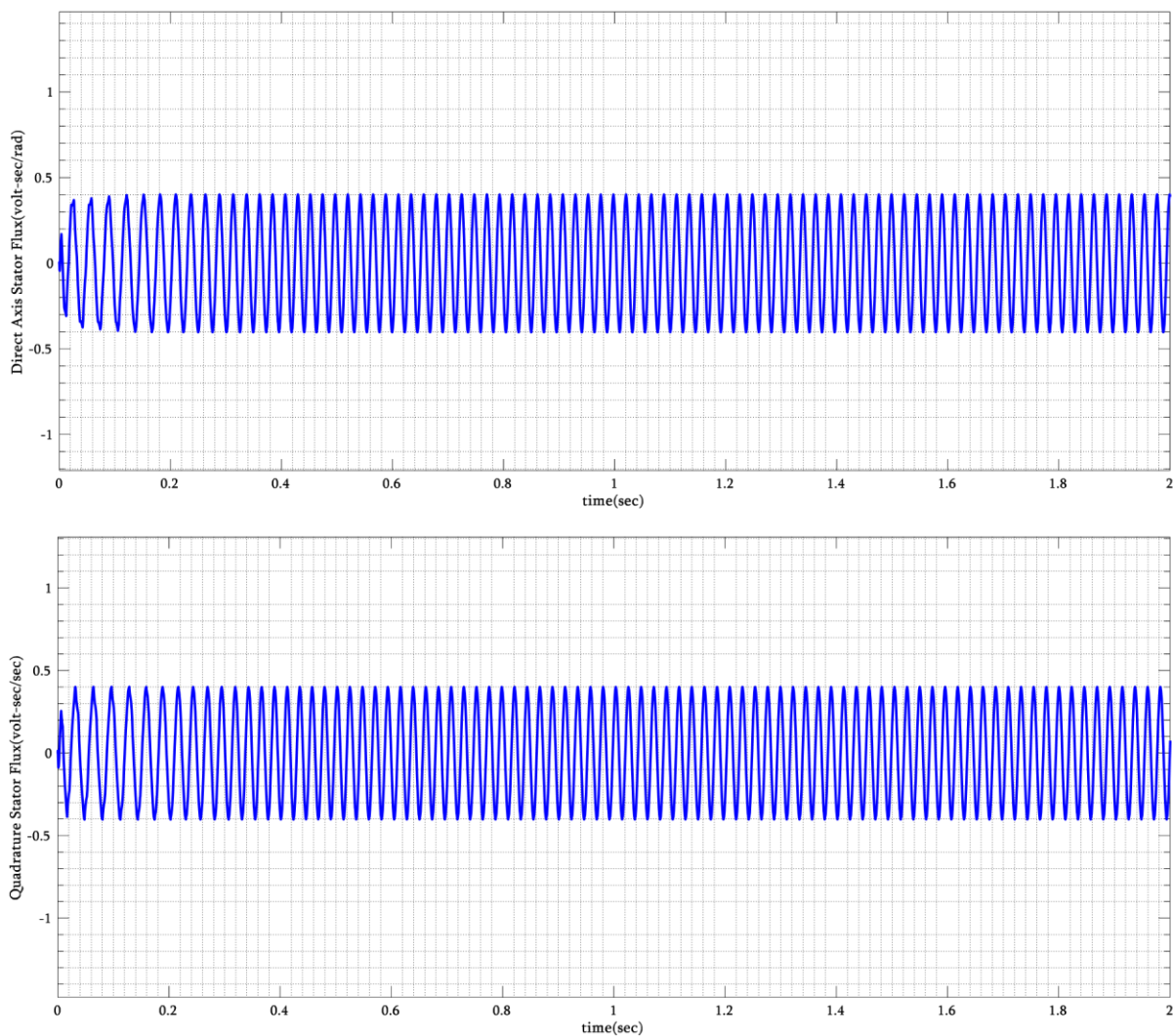
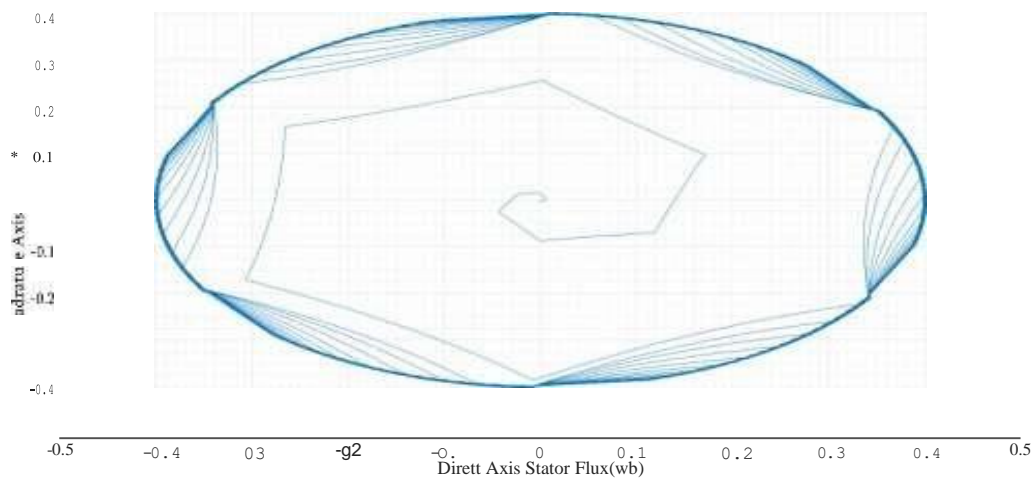


Figure 14: Stationary direct and quadrature axis flux

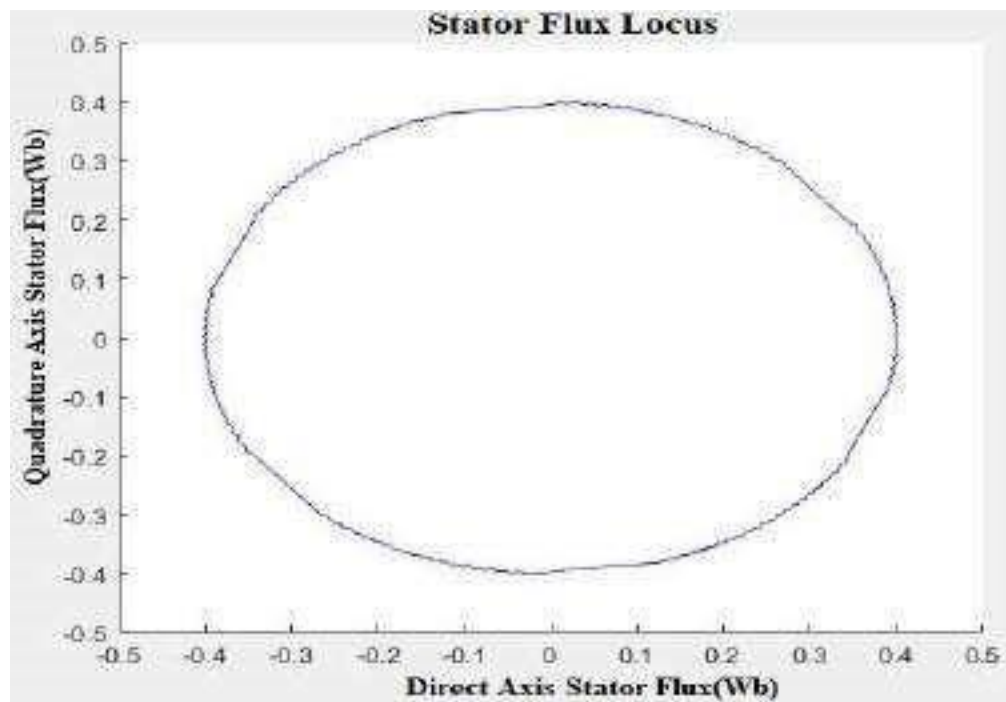
We know synchronous speed frequency is approximately 50Hz, stator flux linkage is directly influenced by this synchronous speed frequency so that we can see from figure 14 we obtained the approximated frequency of 50Hz.



Original Article



(a)



(b)

Figure 15: Stator flux locus(a)Transient flux locus b) Steady-state flux locus)

## Original Article

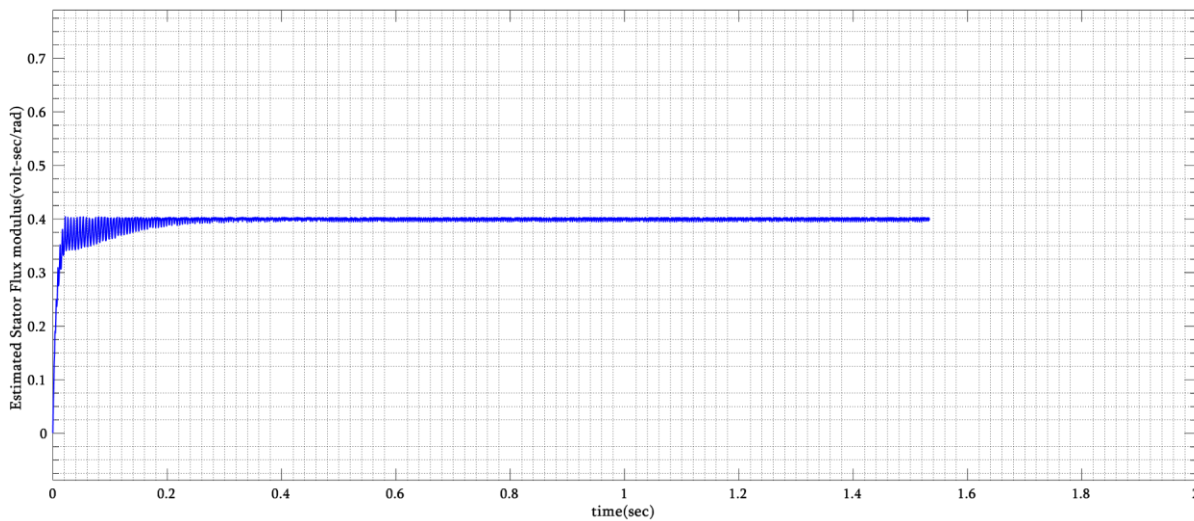


Figure 16: Estimated stator flux modulus

From figure 16, we can see the resultant stator flux value maintained constant throughout the running time and we achieved maximum relative error 0.525%. this error comes due to the presence of the ripple in our estimation. The flux locus in figure 15 indicates that it plots the flux in the direct axis (horizontal) verses in the quadrature axis(vertical). So, the locus must be maintained at the flux reference otherwise the flux estimation technique is not proper.

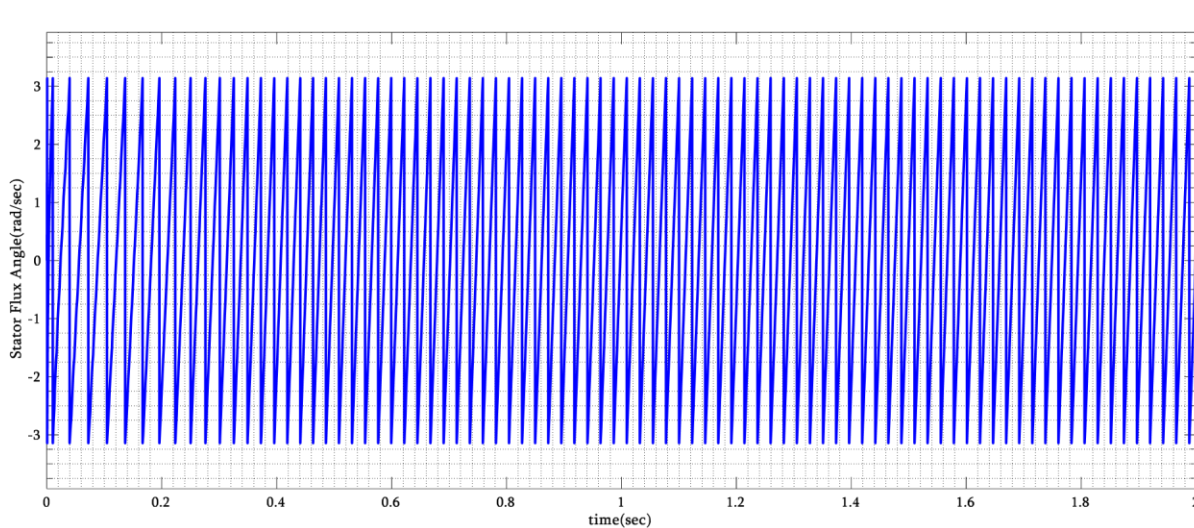


Figure 17: Estimated stator flux angle

When we estimate the stator flux angle, it varies from 0 rad ( $0^0$ ) to  $2\pi$  ( $360^0$ ) and it has approximately a frequency of 50Hz. Arc tangent (atan2) function returns the value from  $-T$  to  $T$ , which covers all quadrants.

Original Article

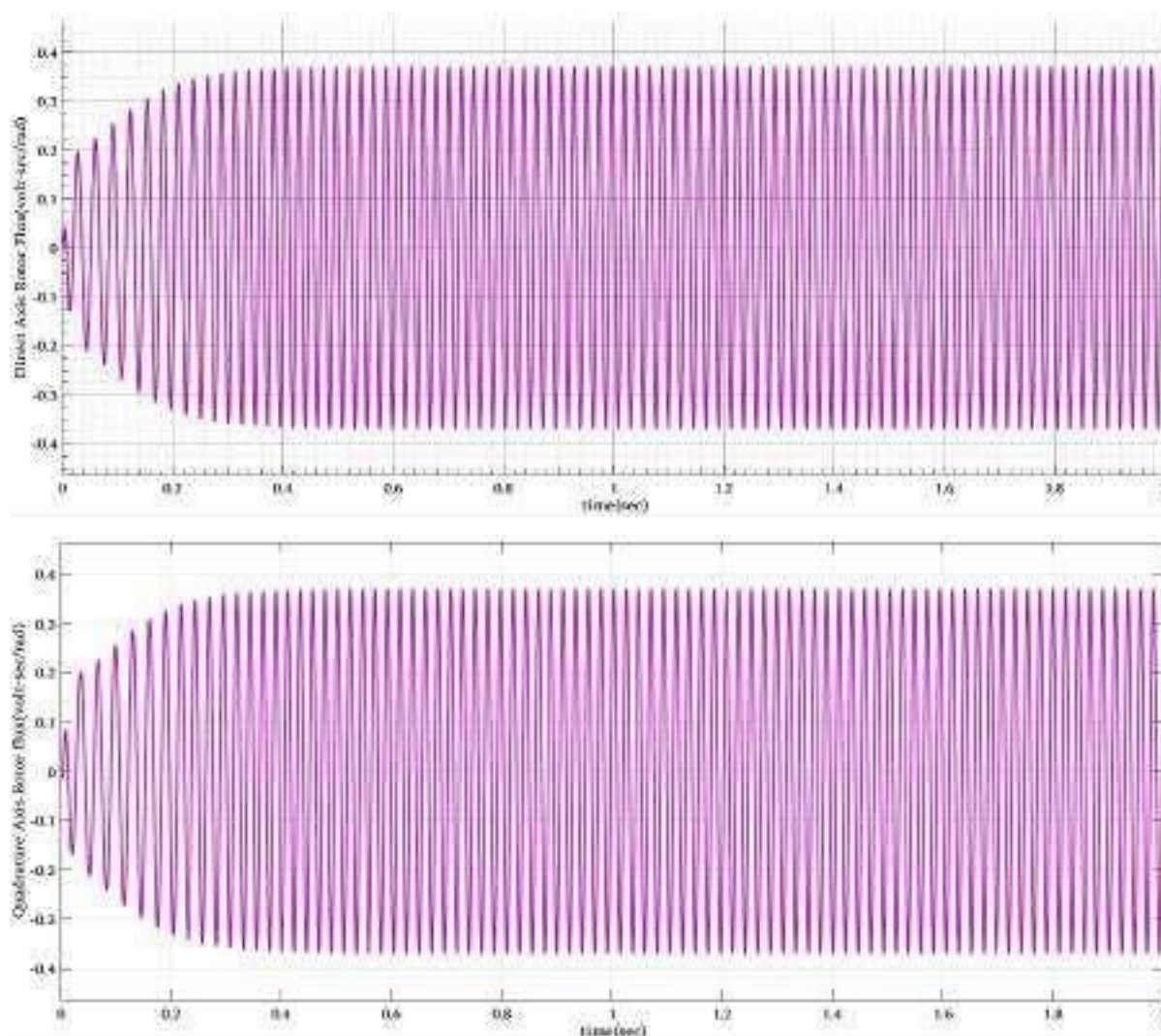


Figure 18: Estimated direct and quadrature rotor flux in the stationary reference frame

# Original Article

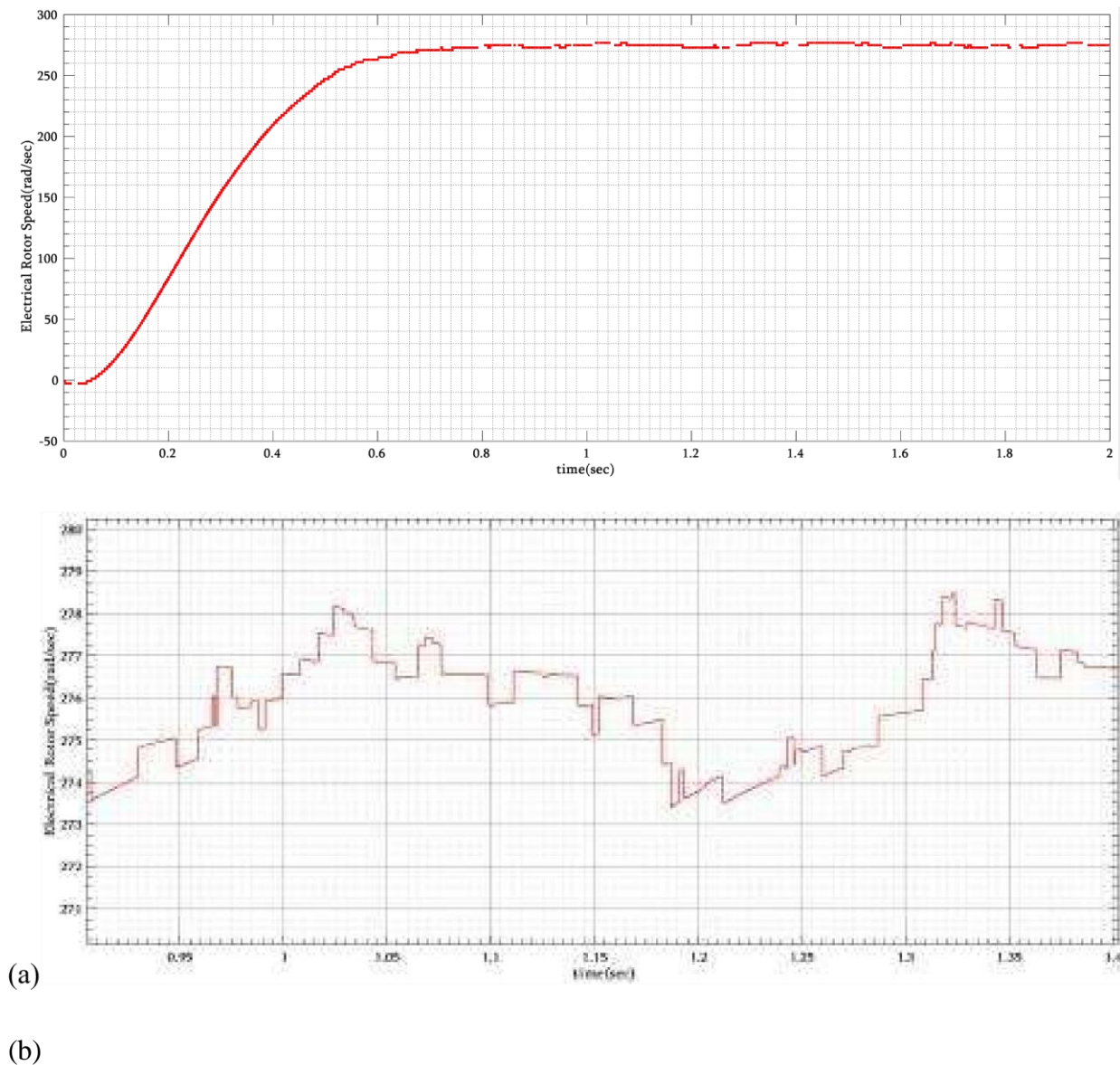


Figure 19: a) Estimated rotor speed without load torque b) rotor speed in zoom view

The reference speed is the step input with value 276  $TTT$ , we got the estimated speed reaches its  $TTT$

reference speed approximately with in a 0.5 second and it remains constant after this time. We also observed that after the speed reaches its reference speed the stator winding currents (approximately sinusoidal waveforms), the direct axis stator flux (has sinusoidal waveforms), quadrature axis stator flux (has sinusoidal waveforms), and the stator flux angle(position) has stable waveforms with a constant frequency.



## Original Article

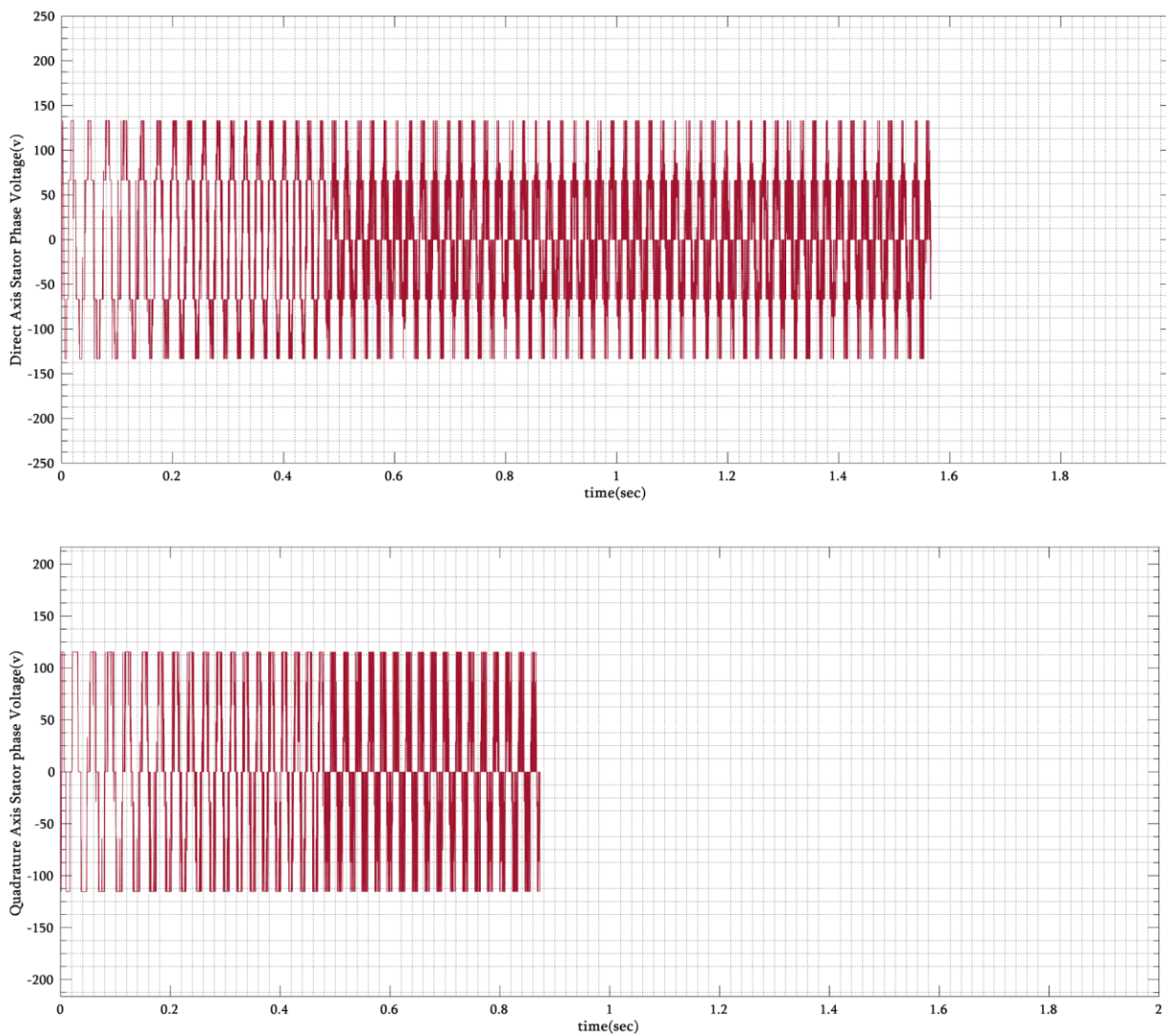


Figure 20: Phase voltage in the stationary d-q axis

From Figure 20 we have direct axis stator voltage and quadrature axis stator voltage with sampling time of 0.0001sec.

## CONCLUSION

The presented work deals with the description of the principle of direct torque-controlled induction motor drive without using a speed sensor (using speed estimation techniques). The stationary frame of reference is used for our analysis during design and modeling our system in MATLAB/Simulink toolbox. The  $T_T - T_T$  modeling procedure and the modeling equation in the direct torquecontrolled induction motor drive with a detailed discussion of achieved result obtained from the simulation model are presented. We could also demonstrate that DTC allows decoupling control of stator flux linkage and electromagnetic torque. when we set reference speed at different values the stator flux must not be changed with respect to the reference speed. This indicate decoupling control of flux and torque; controlling torque means indirectly controlling speed. From MATLAB Simulink the

## **Original Article**

performance of speed response will be further improved by using an appropriate tuning mechanism of PI controller gains.

## **Reference**

P. Vas, "Sensorless Vector and Direct Torque Control", Oxford University Press, 1998.

Ned Mohan, "Advanced Electric Drives: Analysis, Control, and Modeling Using MATLAB/Simulink", 1<sup>st</sup> ed. John Wiley & Sons, Inc., 2014.

Tze-Fun Chan and Keli Shi, "Applied Intelligent Control of Induction Motor Drives", 1<sup>st</sup> ed., John Wiley & Sons (Asia) Pte Ltd, 2011.

A K. Mandal, "Introduction to Control Engineering Modeling, Analysis and Design ", New Age International (P) Ltd., 2006.

Tesfaye Meberate Anteneh, Ayodeji Olalekan Salau, Takele Ferede Agajie, Engidaw Abel Hailu “Design and implementation of a Direct Torque Controller for a Three Phase Induction Motor based on DSP,” International Journal of Applied Engineering Research, Volume 14, Number 22 (2019), pp. 4181-4187